

John C. H. Chiang · Cecilia M. Bitz

Influence of high latitude ice cover on the marine Intertropical Convergence Zone

Received: 16 August 2004 / Accepted: 10 May 2005 / Published online: 21 July 2005
© Springer-Verlag 2005

Abstract We investigate the causes for a strong high latitude imposed ice (land or sea) influence on the marine Intertropical Convergence Zone (ITCZ) in the Community Climate Model version 3 coupled to a 50-m slab ocean. The marine ITCZ in all the ocean basins shift meridionally away from the hemisphere with an imposed added ice cover, altering the global Hadley circulation with an increased tropical subsidence in the hemisphere with imposed ice and uplift in the other. The effect appears to be independent of the longitudinal position of imposed ice. The anomalous ice induces a rapid cooling and drying of the air and surface over the entire high- and midlatitudes; subsequent progression of cold anomalies occurs in the Pacific and Atlantic northeasterly trade regions, where a wind-evaporation-sea surface temperature (SST) feedback initiates progression of a cold SST ‘front’ towards the ITCZ latitudes. Once the cooler SST reaches the ITCZ latitude, the ITCZ shifts southwards, aided by positive feedbacks associated with the displacement. The ITCZ displacement transports moisture away from the colder and drier hemisphere into the other hemisphere, resulting in a pronounced hemispheric asymmetric response in anomalous specific humidity; we speculate that the atmospheric humidity plays a central role in the hemispheric asymmetric nature of the climate response to high latitude ice cover anomalies. From an energy balance viewpoint, the increased outgoing radiative flux at

the latitudes of the imposed ice is compensated by an increased radiative energy flux at the tropical latitudes occupied by the displaced ITCZ, and subsequently transported by the altered Hadley and eddy circulations to the imposed ice latitudes. The situation investigated here may be applicable to past climates like the Last Glacial Maximum where hemispheric asymmetric changes to ice cover occurred. Major caveats to the conclusions drawn include omission of interactive sea ice physics and ocean dynamical feedback and sensitivity to atmospheric physics parameterizations across different models.

1 Introduction

This study stems from a previous paper (Chiang et al. 2003) noting a systematic and strong response of the marine Intertropical Convergence Zone (ITCZ) in an atmospheric general circulation model coupled to a uniform 50-m slab ocean to an imposed increase in the ice cover in one hemisphere. Specifically, the marine ITCZ in all ocean basins shifts meridionally away from the hemisphere with an imposed additional ice extent, altering the Hadley circulation so that there is increased tropical subsidence in the hemisphere with imposed ice and uplift in the other.

This effect was surprising as there is a known tropical influence on the high latitude interannual variability (for example, there is a discernable ENSO influence on high latitude sea ice extent (Yuan and Martinson 2000)), there is little evidence for high latitude ice influence on marine tropical climate variability. However, there is increasing evidence from paleoproxy data and paleoclimate simulations to suggest a linkage between high latitude ice and the marine tropics. High resolution tropical proxy records from the Cariaco basin in the western

J. C. H. Chiang (✉)
Department of Geography and Center for
Atmospheric Sciences, University of California, 547 McCone Hall,
94720-4740 Berkeley, CA, USA
E-mail: jchiang@atmos.berkeley.edu
Tel.: +1-21-5106423900
Fax: +1-21-5106423370

C. M. Bitz
Applied Physics Laboratory, Polar Science Center,
Seattle, WA, USA

tropical Atlantic (e.g., Peterson et al. 2000; Hughen et al. 1996) and Santa Barbara basin in the eastern subtropical Pacific (Kennett and Ingram 1995), both show climate variations that co-vary with ice core $\delta^{18}\text{O}$ temperature record during the last glacial period and Holocene that are recorded in the Greenland Ice Sheet Project II (GISP II—Stuiver and Grootes 2000). In particular, features in the tropical and subtropical records appear to coincide with abrupt climate changes in the GISP II record that are associated with the Dansgaard-Oeschger (D/O) events and deglaciation (Lynch-Stieglitz 2004). Insofar as the GISP II isotope record can be interpreted to originate from changes to northern high latitude land ice or sea ice extent, it implies a connection between ice cover and the marine tropical climate. A recent atmospheric general circulation model (AGCM) study (Li et al., submitted) shows that relatively small displacements in the North Atlantic sea ice edge (presumably in response to an altered North Atlantic thermohaline circulation) can easily explain the abrupt changes to temperature recorded at GISP II, lending credence to the postulated role of sea ice in abrupt climate change. Moreover, the timing of the Younger Dryas variations in the Cariaco basin appears synchronous with the GISP II record (Hughen et al. 2000, Lea et al. 2003), suggesting that the high-to-low latitude connection can be rapid. A teleconnection established by the fast-adjusting atmosphere is consistent with this observation, although ocean dynamical mechanisms (e.g., as proposed by Yang 1999) can act relatively quickly as well.

The seminal Last Glacial Maximum (LGM) model study by Manabe and Broccoli (1985) using the Geophysical Fluid Dynamics Laboratory (GFDL) model with slab ocean demonstrated that the land ice boundary conditions could affect the tropical climate. They focused on an interhemispheric asymmetry in their slab ocean model in response to the LGM land ice, with the northern hemisphere cooling significantly but the southern hemisphere temperature not significantly responding, indicating that the atmosphere primarily locally balances the radiative forcing introduced by the ice sheets. While they did not analyze in any significant detail the reflection of interhemispheric asymmetry in the tropics, the southward displacement in the ITCZ, and the meridional gradient in sea surface temperature (SST) anomaly near the equator are quite apparent from their surface wind response. In a more recent study with an updated and higher resolution GFDL model, Broccoli (2000) also noted considerable spatial variability in tropical surface circulation and surface air temperature response to LGM boundary conditions (incorporating all LGM boundary conditions, not just land ice) and suggested that this may be, in part, a result of the interhemispheric asymmetry introduced by the land ice influence. In particular, he suggested that the interhemispheric asymmetry leads to a reorientation of the Hadley circulation, with northerly cross-equatorial flow anomalies and a southward-displaced rising branch of the Hadley circulation. Chiang et al. (2003) indeed

shows this to be the case for the tropical Atlantic, showing that most of the tropical circulation anomalies in an LGM simulation in the Community Climate Model version 3 (CCM3) coupled to a slab ocean model are directly attributable to the land ice influence, as opposed to the direct effects of orbital or greenhouse gas changes.

Modern climate variability analogues show that the meridional position of the marine ITCZ is sensitive to perturbations. The boreal spring Atlantic ITCZ meridional position varies interannually in response to anomalous hemispheric gradients in Atlantic SST (e.g., Hastenrath and Heller 1977). Furthermore, this ITCZ response is quite sensitive, shifting position by hundreds of kilometers in response to relatively small SST gradient anomalies ($\sim 1^\circ\text{C}$ between 15°N and 15°S). This sensitivity is also demonstrated in model simulations: e.g., Schneider et al. (1997) shows a significant Pacific ITCZ meridional displacement to meridional SST gradient changes caused by a doubled CO_2 experiment in an AGCM—slab ocean model, but with the SST in the Pacific cold tongue region fixed to a prescribed level. Recognizing this sensitivity, Chiang et al. (2003) proposed that marine meridional ITCZ displacements are a preferred way for the tropics to respond during paleoclimate changes. An interesting feature of the ITCZ displacements in the simulations shown here is that they do not appear to be caused by an externally-imposed change to magnitude of the subtropical trades, a well-known cause of tropical Atlantic interannual ITCZ variability (e.g., Nobre and Shukla 1996). These peculiarities suggested new and interesting climate physics that are yet to be elucidated in the literature.

This study investigates how the CCM3-slab ocean model marine ITCZ adjusts to imposed ice cover changes in the high latitudes. The mechanism for communication from the midlatitudes to the marine ITCZ latitudes turns out to be a coupled feedback between wind, evaporation, and SST (WES feedback) in the region of the northeasterly trades leading to a progression of cold SST anomalies to the tropics; a mechanism previously proposed in the context of tropical Atlantic variability by Xie (1999). Once the cold SST anomalies reach the ITCZ latitudes, the ITCZ displaces away from the hemisphere with the imposed ice cover, aided by positive feedbacks associated with the displacement. We also speculate that the particular response of atmospheric moisture plays a significant role in the hemispheric asymmetric nature of the climate response to an added ice cover in one hemisphere. The exclusion of ocean dynamics in the model and the vulgarities of this particular model's parameterizations may well mean that the mechanism underlying this influence may not have a direct bearing on reality. However, the fact remains that this is a typical model used for simulating earth's climate and that its tropics distinctly feels an influence that originates thousands of kilometers away. It is worthwhile understanding how this comes about and in the process gain insight on if and how this

mechanism can manifest itself in the real world. In this vein, we also explore how this mechanism may be manifested in the observed modern and paleoclimate record.

Our paper proceeds as follows. The model and its configuration that we use are introduced in Sect. 2. The result of simulations with imposed increased northern sea and land ice extent is discussed in Sect. 3. We will show that the anomalies possess zonally symmetric characteristics, which motivates us to examine the zonal mean anomalies. To better understand the response, we examine the transient response of the model to the imposition of sea ice (Sect. 4). Based on these results, we propose a mechanism for high latitude ice influence (Sect. 5) on the marine ITCZ. In Sect. 6, we discuss the applicability of this mechanism in the real world, in particular regarding its applicability to the modern and paleo climate variability.

2 Model description

The model setup used is essentially the same as in Chiang et al. (2003). We use the Community Climate Model version 3 (CCM3), general circulation model, (Kiehl et al. 1998) that has been used extensively in simulations of the present-day and past climates. It is coupled to a 50-m fixed depth ocean mixed layer that allows thermodynamic atmosphere-ocean interactions, but no ocean dynamics. Our simulations are done in T31x15 resolution (31 basis functions in the meridional dimension and 15 for the zonal, equivalent to 48 longitude and latitude grid points). It is somewhat coarser than the standard T42 resolution of the model, but the coarser resolution has been demonstrated successfully to simulate the extratropical (Yin and Battisti 2001) and tropical climate (Biasutti 2000; Chiang et al. 2003) and allows an order of magnitude increase in model throughput relative to the CCM3 standard resolution. The faster throughput allows us to experiment with various boundary conditions for testing hypotheses, without unduly sacrificing realism.

Our control run has imposed modern-day orbital, greenhouse gases, sea ice, and land surface conditions. A flux correction Q (hereafter referred to as the Q -flux) is applied to the surface ocean fluxes to force the slab ocean to follow the present-day SST monthly mean climatology:

$$\rho_o C_o h_o \frac{\partial T}{\partial t} = F + Q \quad (1)$$

where ρ_o is the density of seawater (taken to be $1.026 \times 10^3 \text{ kg/m}^3$), C_o is the specific heat capacity at constant pressure ($3.93 \times 10^3 \text{ J/K.kg}$), h_o the mixed layer depth, and F the net surface flux into the ocean. Q is derived from an uncoupled simulation using fixed climatological monthly mean SST (Kiehl et al. 1996):

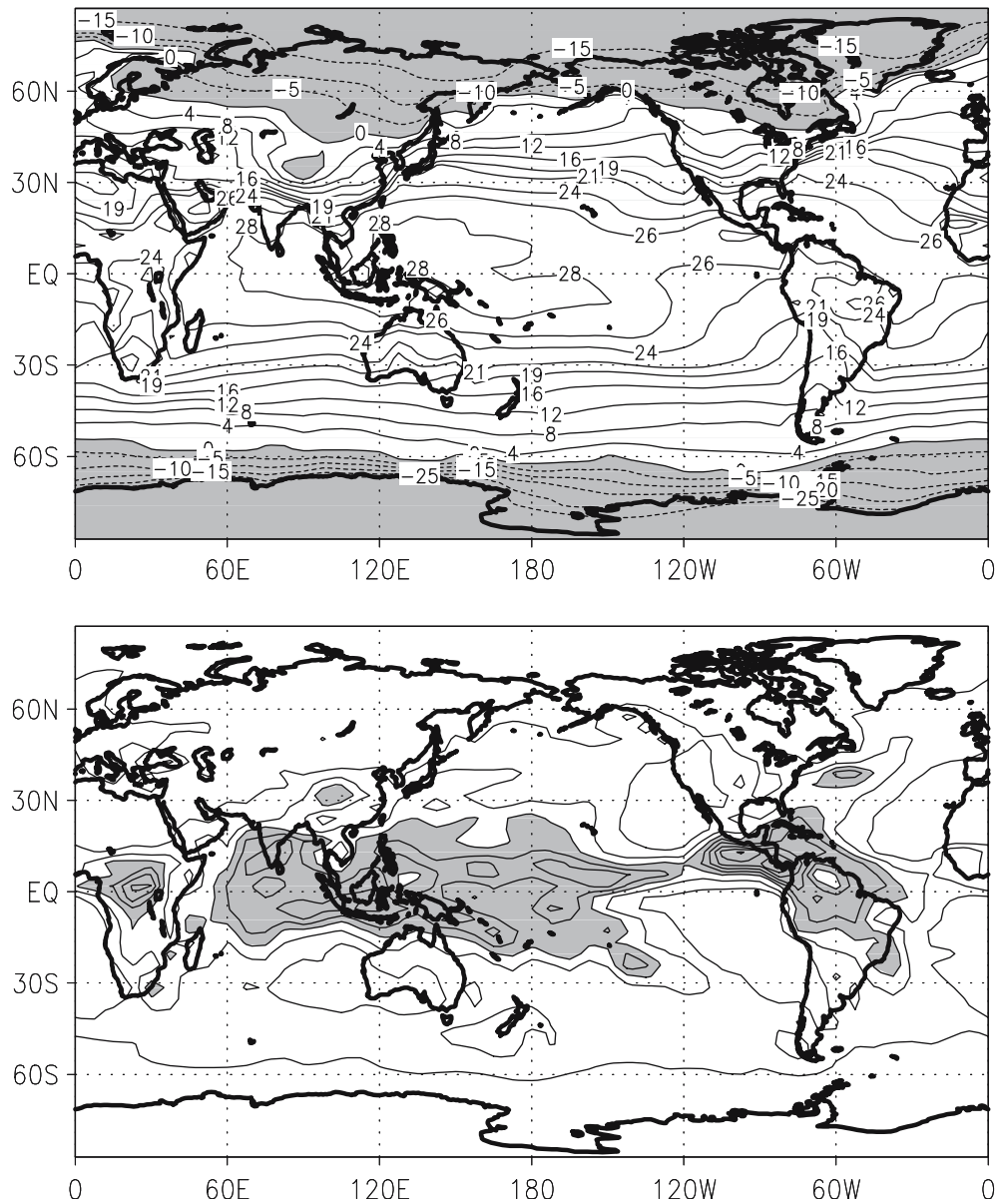
$$Q^m = \rho_o C_o h_o^m \frac{(T^{m+1} - T^{m-1})}{(d^{m+1} - d^{m-1})} - F^m \quad (2)$$

where T^m is the climatological monthly mean SST and F^m is the monthly mean net surface flux derived from that same run. In our case, the F^m is averaged over 30 years. The monthly mean Q^m values are linearly interpolated to obtain the instantaneous Q required in Eq. 1. We interpret the application of the Q -flux as the imposition of the modern-day ocean heat transport convergence, though in reality it also corrects for model bias.

Sea ice coverage is prescribed to be annually periodic from a monthly mean climatology. The sea ice thickness is set to 2 m everywhere with a snow depth of 5 cm year-round. Imposing the sea ice coverage maintains its compatibility with the imposed Q -flux, which is computed from a fixed climatological SST run with the same sea ice coverage, so the climate of the control slab ocean run is very close to that of the fixed-SST simulation. However, because sea ice is not interactive, we impose the additional condition that the open ocean temperature is always above the model sea ice freezing temperature threshold of -1.7999°C . This necessary but unrealistic constraint has some rational basis: in the absence of sea ice formation, surface ocean points that experience cooling when at or near the freezing temperature are often subject to open ocean convection, and any further temperature drop could be arrested by the heat exchange with the interior ocean, which we can assume to be an infinite heat source for the purpose of our exercise. In practice it means that any ocean point exercising the SST minimum constraint is a temporary source of heat to the atmosphere. This SST constraint is exercised in our simulations by ocean SST points in the neighborhood of imposed sea ice points. There is a complementary sink of heat from the atmosphere in regions where the net surface fluxes is positive into the ice. Normally this would cause the ice to melt, but this is not allowed in our integrations because the ice thickness is prescribed. Given that we do not have interactive sea ice, our simulations should be viewed as sensitivity studies, much like the way others have studied atmospheric circulation sensitivities to (say) imposed sea surface temperature perturbations. We note that other studies (e.g., Deser et al. 2004) have also investigated atmospheric circulation changes to imposed sea ice anomalies.

A control climatology is simulated by running the CCM3 50-m slab over 35 years, discarding the first 15 years as spinup and averaging over the last 20 years to obtain the climatology. The control run SST and precipitation is shown in Fig. 1. The SST simulation is good, as expected by construction. The precipitation climatology shows a reasonably realistic distribution though with a somewhat diffuse marine ITCZ, nonetheless it is sufficiently realistic for our purposes.

Fig. 1 The annual mean **a** SST and surface land temperature (in °C) and **b** precipitation (in mm/day) in the CCM3-slab ocean control run. For surface temperature, regions below 0°C are shaded. For precipitation, the contour interval is 1.5 mm/day, and regions larger than 4.5 mm/day are shaded



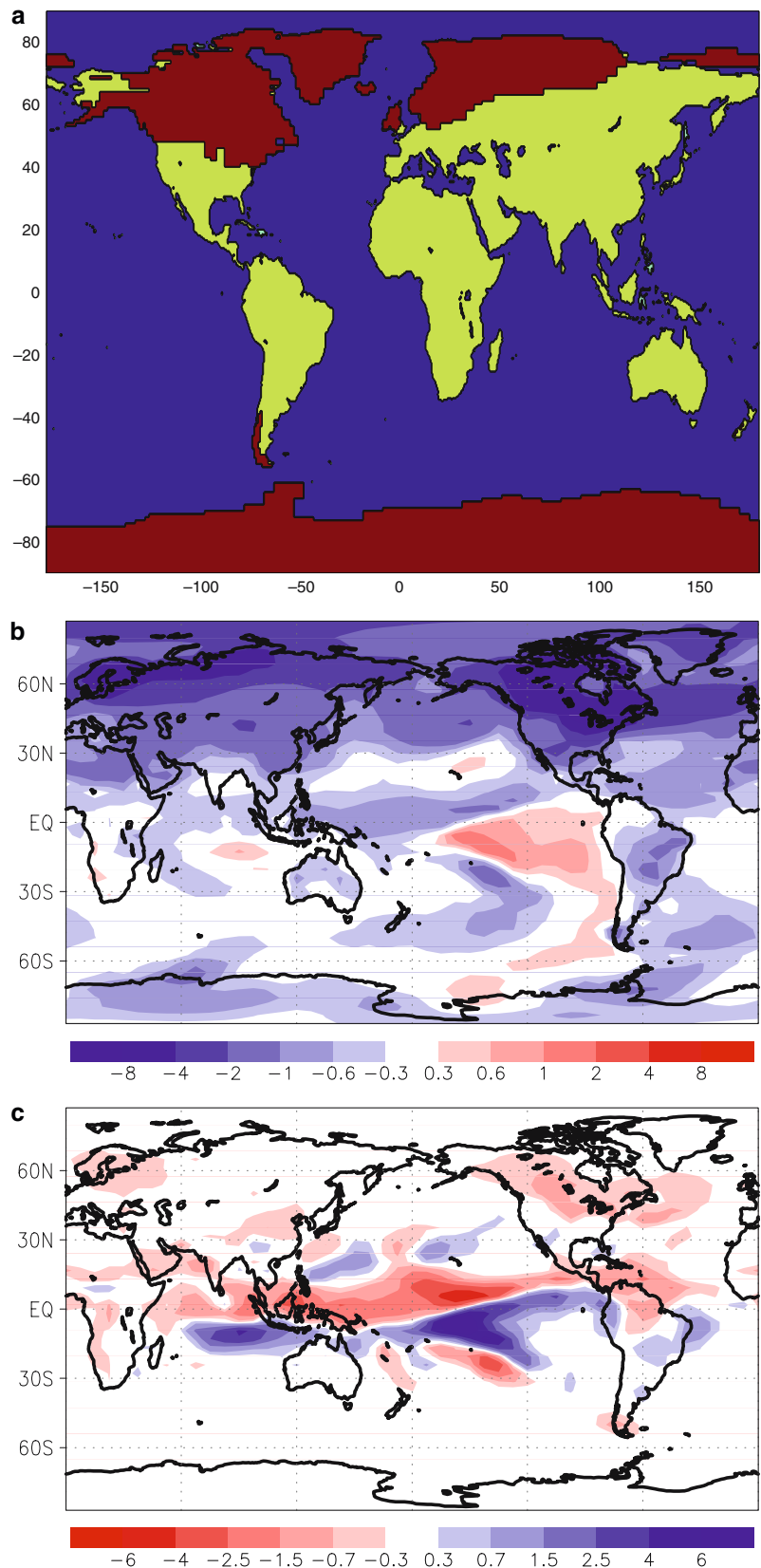
3 Results of simulations with increased northern hemisphere ice

3.1 Precipitation and surface temperature

We first examine a simulation with an LGM land ice distribution (shown in Fig. 2a), but with zero ice thickness (i.e., no change in surface orography, so only the land surface effects, in particular the ice albedo, was included) was imposed over all present-day land points. The length of the integration is treated as the same for the control—35 years, discarding the first 15 years as spinup and using the last 20 years for the climatology. The same orbital configuration, sea ice coverage, and Q -flux were used as in the control. The LGM land ice cover distribution comes from a reconstruction by

Peltier (1994) and is predominantly in the northern hemisphere (NH) and is essentially a NH forcing. The additional land ice shifts the ITCZ in all three marine ocean basins unmistakably southwards, and there is a widespread cooling in the NH surface temperature, especially in the high latitudes over the positions of the additional ice (Fig. 2b, c). The southern hemisphere (SH) surface temperature and the position of the land ITCZ remain relatively unchanged by comparison. The interhemispheric asymmetry in the response of land surface temperatures to land ice has been previously elaborated by Manabe and Broccoli (1985). A two-sided t -test shows that the ITCZ displacements in the Pacific and Atlantic basins are statistically significant at the 95% level (not shown), as is the temperature change over most regions in the NH. Much of the surface

Fig. 2 **a** LGM land ice extent (in red). **b** and **c** Annual mean differences between the LGM land ice albedo and present-day simulations. **b** SST and surface temperature (in K) and **c** precipitation (mm/day). The difference shows a significant southward shift of the marine ITCZ in all the three ocean basins in the LGM land ice albedo simulation. The same perturbation simulation using a finer T42 resolution gives qualitatively similar results, although the magnitude in the precipitation response is not as pronounced



temperature change in the SH is also statistically significant, even though the amplitude of the changes are small. The effect on the land ice on the marine ITCZ

does not apparently depend on model resolution: a similar LGM land ice experiment using the higher T42 resolution (not shown) exhibits similar anomalies in

both surface temperature and precipitation, although the magnitude of the marine precipitation change is less pronounced, especially over the equatorial Indian ocean.

Imposing anomalous NH sea ice, as opposed to land ice, has a similar effect. We impose it as done in Chiang et al. (2003), but applied only to the northern hemisphere (Fig. 3a—additional details for how this distribution was derived can be found in the above reference). Sea ice is added in the NH high latitudes during most months of the year, peaking in the NH winter season. The result (Fig. 3b, c) is qualitatively and quantitatively similar to the simulation imposing LGM land ice extent, with the marine ITCZ in all three basins shifting to the south. The spatial structure of the surface temperature response (Fig. 3b) differs in the high northern latitudes compared to the land ice simulation, since the largest cooling occurs over regions of imposed land/sea ice. However, the temperature structure, south of 30°N, is quite similar with a striking correspondence of the anomalously cooler and warmer regions. The tropical precipitation response (Fig. 3c) in the sea ice simulation resembles that for the land ice simulation even more markedly, with the southward ITCZ displacement in all the three ocean basins and relatively little response over land regions in the annual mean. We interpret the above result to mean that the mechanism of high-to-low latitude communication is essentially the same in the land and sea ice simulations.

We note that the imposition of sea ice is not simply an albedo effect. Sea ice paves over former ocean points that previously stored heat seasonally and also provided heat to the atmosphere through imposed ocean heat transport convergence (we do not replace the lost Q -flux by redistributing it). Sea ice is a good insulator, and hence its surface temperature during winter is typical of land surfaces. In addition, evaporation from sea ice is usually much smaller than from ice-free ocean. In winter, compared to ice-free ocean, the air overlying sea ice is typically cooler, drier, and equilibrates faster.

Our result is insensitive to the ocean basin in which sea ice is imposed. We performed two additional experiments imposing the same NH additional sea ice, but confined only to the Atlantic and to the Pacific sectors respectively. In both cases, the ITCZ shifted southwards in all the three ocean basins. The result is also insensitive to the hemisphere where sea ice is imposed. We repeated the same experiment but imposing additional sea ice in the southern hemisphere—the sea ice anomalies were derived using the same procedure to derive the northern anomalies. In this case, the ITCZ displaces northwards in all the three ocean basins (not shown).

3.2 Zonal mean response

The relative zonal symmetry in the high latitude temperature and marine ITCZ response suggests examination of zonal mean changes as a useful simplification.

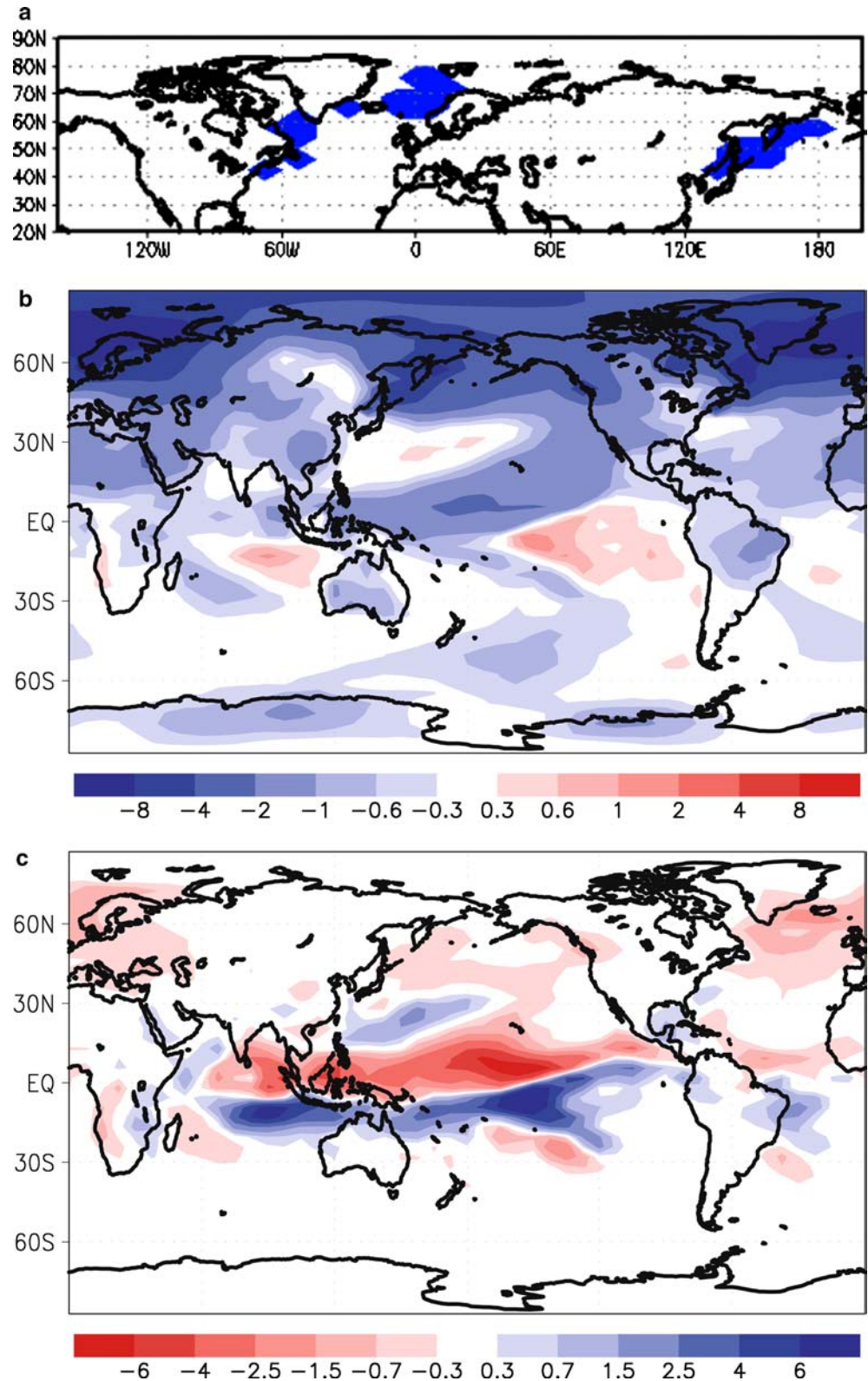
The fields shown in this subsection are for the T31×15 LGM land ice simulation; the results are qualitatively similar for the NH sea ice simulation. The annual and zonal mean air temperature change (Fig. 4a) exhibits cooling almost everywhere, in particular the high northern latitudes, where the magnitude is up to and beyond 3 K in the lower troposphere. Away from the high- and mid-northern latitudes (equatorwards of 30°N), the cooling is significant but relatively small (between 0 K and 1 K). We also point out that the tropical hemispheric asymmetry near the equator seen in the precipitation response does not appear to be strongly reflected in tropical air temperature, not surprisingly as the large-scale atmospheric dynamics acts to dampen tropical tropospheric temperature gradients (e.g. Schneider 1977).

In contrast, the atmospheric moisture content exhibits pronounced hemispheric asymmetry. The zonal and annual mean specific humidity (Fig. 4b) in the NH hemisphere is substantially drier, while the SH is slightly moist in the tropical latitudes. The dry anomaly in the NH is focused over two regions, in the mid-to-high latitudes centered around 55°N, and in the northern tropics centered around 10°N. The magnitude of change generally exceeds 0.3 g/kg in the northern extratropics above 700 mb and can reach up to 0.8 g/kg near the surface at around 40–50°N, which is a substantial change considering that the mean specific humidity at 50°N on the surface is only around 6 g/kg. A relative minimum in the specific humidity anomaly occurs at around 30°N, but then picks up again in the deep northern tropics, with decreases maximizing around –0.6 g/kg in the lower mid-troposphere (~700 mb).

The tropical changes to the specific humidity reflect changes to the Hadley circulation. A relatively sharp gradient in the SST anomaly occurs over the equator (Fig. 4c), consistent with the southward displacement of the ITCZ, with a ~0.5 K reduction in the NH tropics (0–30°N) and relatively little change in the SH tropics (0–30°S). The mean meridional circulation changes with anomalous uplift just south of the equator and subsidence just to the north of it (Fig. 4d). The anomalously drier conditions in the northern tropics come primarily through the total advection tendency (figure not shown), presumably through the subsidence of drier upper tropospheric air. Also, the annual and zonal mean cross-equatorial meridional water transport anomaly (Fig. 4e)—i.e., the difference between the perturbation and control values for $[\overline{qv}]$ where q is the specific humidity, v the meridional velocity, [...] denotes zonal average and the overbar the annual mean—in the atmospheric boundary layer increases southwards by over 12 (g kg⁻¹).(ms⁻¹) with no compensating transport above the boundary layer. The anomalous circulation causes the anomalously drier hemisphere to feed moisture into the anomalously moist hemisphere. We discuss the significance of this statement in Sect. 6.

The imposed ice dramatically changes the top of atmosphere (TOA) radiative balance and the poleward

Fig. 3 a Distribution of additional sea ice for January, from Chiang et al. (2003). There is no anomalous sea ice in the northern hemisphere in July. **b, c** As in Fig. 2b and c, respectively, but for the case of imposed sea ice



atmospheric energy transport. Increased albedo in the higher northern latitudes results in decreased zonal and annual mean incoming SW at TOA reaching a peak magnitude of around -0.25 GW/m summed over the latitude band (Fig. 5a) of which only about half is

compensated for by the reduced outgoing longwave radiation (OLR) (Fig. 5b). In the tropics, the changed radiative balance reflects the displacement in the ITCZ with the effects dominated by increased OLR in the anomalously drier northern tropics partly compensated

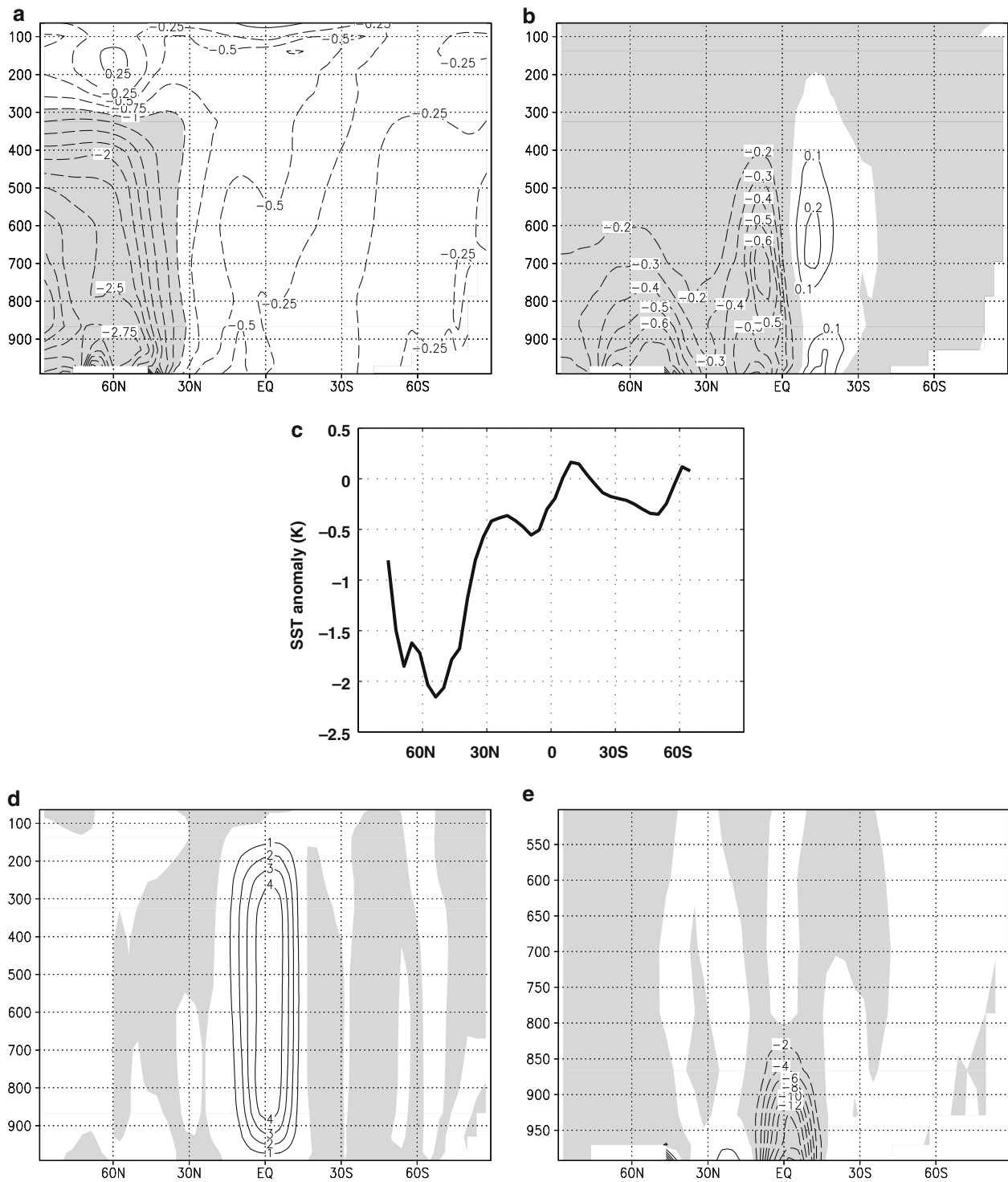


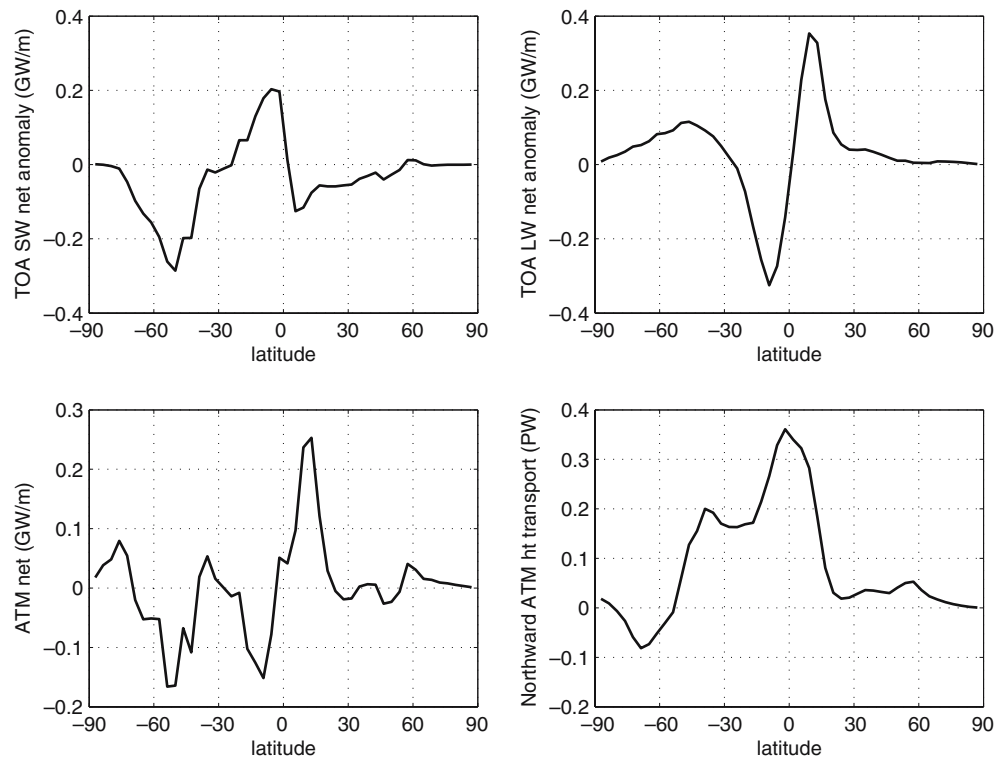
Fig. 4 Zonal and annual mean differences between the LGM land ice simulation and control; **a** air temperature (contour interval 0.25 K, regions below -1 K are shaded), **b** specific humidity

(contour interval 0.1 g/kg, negative values are shaded, zero contour omitted); **c** SST (K), **d** mean meridional circulation ($\times 10^{10}$ kg/s, negative values are shaded, zero contour omitted), **e** meridional

for by the increased incoming SW at TOA; and reduced OLR in the anomalously wetter southern tropics again partly compensated for by the reduced incoming TOA shortwave radiation. The change to the zonal and

annual mean net energy absorbed by the atmosphere in the LGM land ice simulation (Fig. 5c)—calculated by subtracting the net energy flux at the surface from the net flux at the top of the atmosphere (TOA)—show a

Fig. 5 Annual mean energy flux summed over latitude bands, and zonal and annual mean atmospheric heat transport differences between the LGM land ice simulation and control. **a** TOA shortwave flux (GW/m, positive values are towards the surface), **b** TOA longwave flux (GW/m, positive values are towards the surface), **c** total energy absorbed in the atmospheric column (GW/m), **d** total northward energy transport by the atmospheric circulation (PW)



redistribution of energy absorbed by the atmosphere with a substantial increase in the southern tropics (0–20°S), and small increases in the northern subtropical (around 30°N) and polar regions (around 80°N), accompanied by decreases in the northern tropics (around 15°N) and northern mid-to-high latitudes (around 55°N). This redistribution is almost entirely due to the radiative changes at the TOA: changes to the annual mean surface fluxes summed over latitude bands are basically zero everywhere except for small changes (less than 0.05 GW/m) in the high northern and southern latitudes where the fixed lower bound of -1.7999°C on the SST, and also the fixed interior ocean temperature used in the sea ice heat flux calculation, imparts a small energy input into the atmosphere.

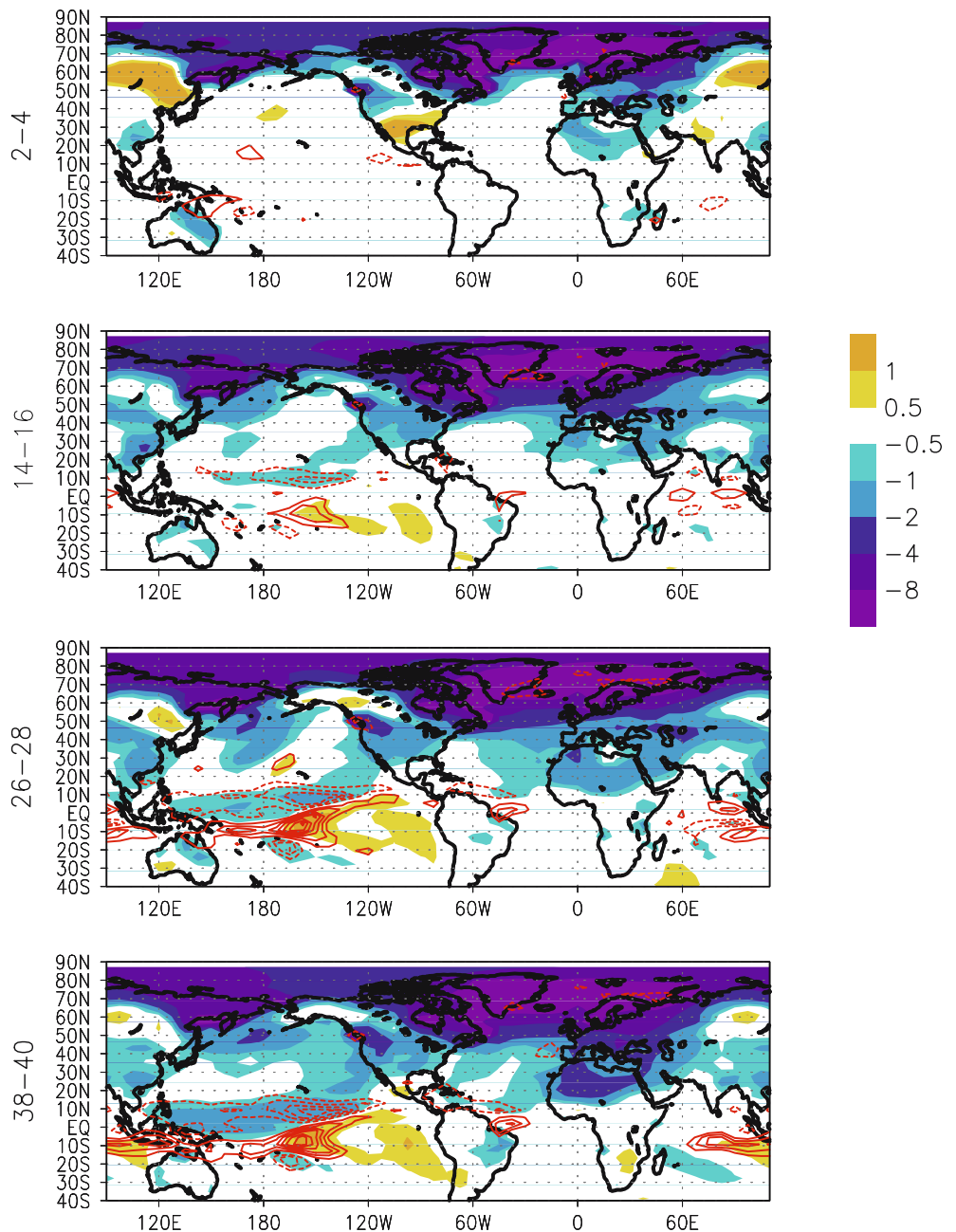
In the global and annual mean, the global TOA shortwave flux towards the earth decreases by 0.66 PW, and compensated for by a 0.56-PW reduction to the OLR and 0.1 PW from the surface heating at high latitudes. The zonal and annual mean atmospheric energy transport (Fig. 5d)—whose structure is determined primarily by radiative changes at the TOA—shows a substantial (~ 0.35 PW) increase to the northward atmospheric transport over the equator, of which a portion is lost (energy convergence) in the northern tropics and again in the northern midlatitudes (around 50°N). We defer our interpretation of the altered energy budget to Sect. 5, when we introduce a mechanism for the high latitude influence on the tropical marine ITCZ.

4 Transients and surface flux analysis

How does the high latitude ice influence reach the tropics? We examine the adjustment process using CCM3-slab ocean ensemble simulation with ten members, where anomalous NH sea ice cover (the same anomalies as discussed in Sect. 2 and Fig. 3) is abruptly introduced in 1 September of year 0. Each ensemble member was started from a different initial 1 September atmospheric and sea surface temperature conditions (obtained from the control simulation), and run out for 6 years during which the climate has mostly adjusted towards the new equilibrium state. We constructed the baseline climatology by running another ten-member ensemble with the same initial conditions, but without the sea ice cover anomalies. The anomalous fields we show in this section are monthly mean differences between the two ensemble means.

Transients associated with surface temperature (Fig. 6, top panel) show rapid initial cooling of up to and over 8 K of the entire high northern latitudes occurring within the first 3 months from onset. The cooling steadily migrates southwards over the subsequent 2–3 years (Fig. 6, panels 2–4), although the cooling already penetrates into the northern tropical Pacific after the first year. The northern subtropical Pacific SST cooling exhibits a distinct structure coincident with the spatial footprint of the northeasterly trades. Similar behavior is seen with the boundary layer specific humidity, with dry anomalies coincident with

Fig. 6 Surface temperature anomalies (in K) in the transient experiment at 1–3 months (*top panel*), 13–15 months (*middle*) and 25–27 months (*bottom*) beyond the onset of northern hemisphere sea ice anomalies. Note that these months correspond to September through November of each year. Also shown (*red contours*, contour interval 1.5 mm/d) is the anomalous precipitation

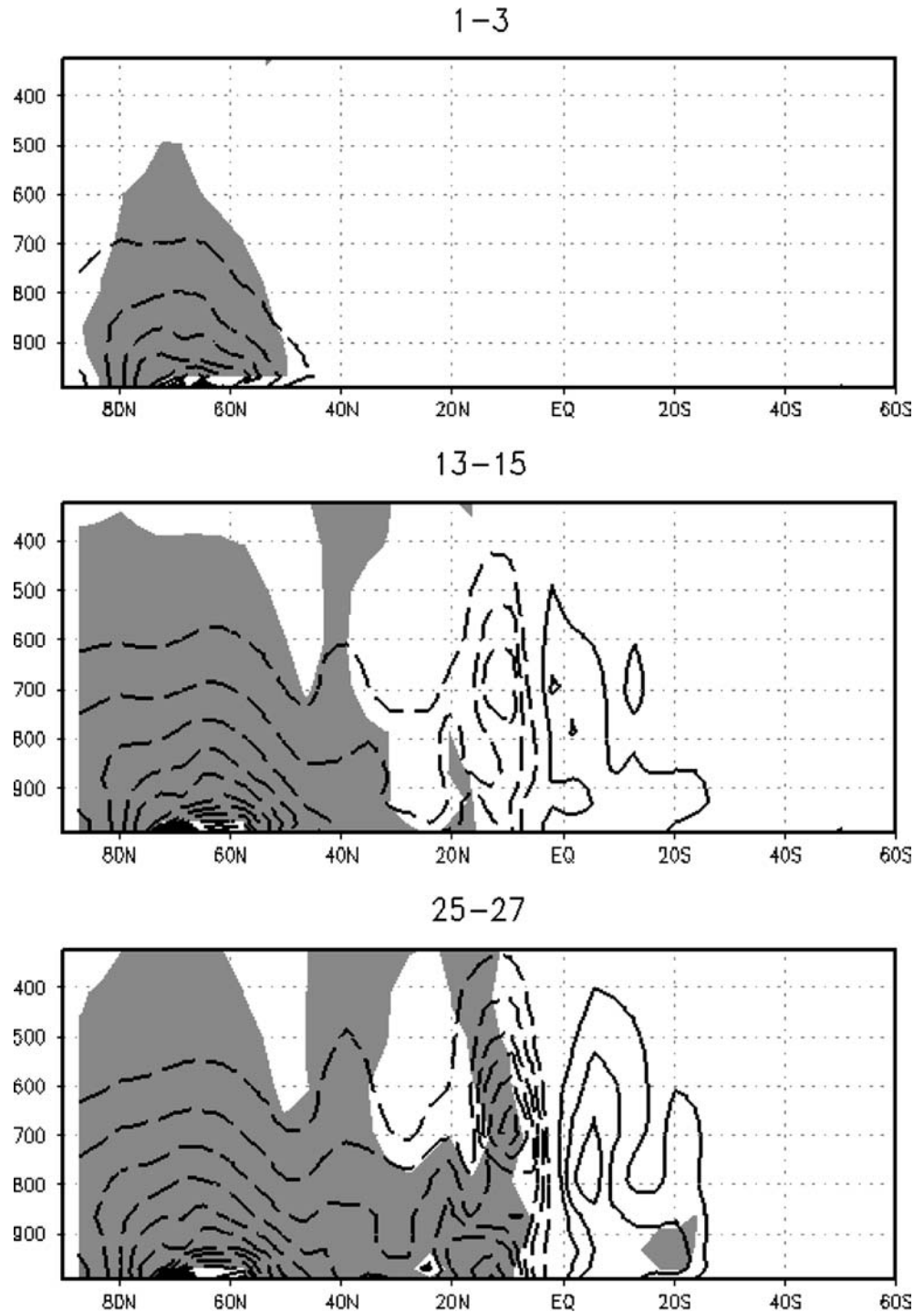


the sea surface temperature cooling (not shown). A similar footprint coincident with the northeasterly trades occurs in the subtropical Atlantic, although it is more readily apparent when viewing the annual mean anomalies (see Figs. 2, 3, for example) than in the September–November anomalies shown in Fig. 6. Once the SST anomalies reach the marine ITCZ latitudes, the southward displacement of the ITCZ occurs (Fig. 6, red contours). The transient signal from the high-to-low-latitudes is also prominent in the humidity content in the atmosphere. The anomalous zonal mean tropospheric moisture content shows prominently the equatorward progression and ITCZ response (Fig. 7). In particular, once the ITCZ displacement sets in, the hemispheric

asymmetry in moisture content anomalies sets in as a consequence of the altered moisture transports by the anomalous Hadley circulation.

The high-to-low latitude communication leading up to the marine ITCZ displacement thus appears linked to the progression of SST anomalies along the subtropical oceans, in particular the northeasterly trades. We simplify the situation by examining anomalies zonally averaged over the ocean, and averaged in 3-month chunks. The Hovmöller plot of the SST anomalies (Fig. 8a) confirms the southward progression of the cool SST anomalies; as a visual aid, we outline its -0.2 K and -0.1 K contours (dashed) in subsequent Hovmöller plots to indicate the leading edge of the cooling. The

Fig. 7 Zonal mean specific humidity anomalies corresponding to the times in Fig. 5 after northern hemisphere sea ice onset, showing the equatorward propagation of dry anomalies and hemispheric asymmetry after ITCZ displacement. The contour interval is 1×10^{-5} g/kg, dashed contours are negative, solid contours positive, and the zero contour is not shown. The grey shaded regions indicate significance at the 95% level, using a two-sided t test



progression of the SST ‘front’ leads to a pronounced southward ITCZ displacement around 12–15 months after the sea ice is advanced (Fig. 8b). The analysis is made more complicated by the seasonal dependence of the precipitation anomalies (which track the seasonal migration of the ITCZ), but the onset of the displacement is clear.

How do the SST anomalies progress to the ITCZ latitudes? The zonal mean net surface flux anomalies over the oceans (Fig. 9a) show that heat is generally

extracted from the northern midlatitude and tropical oceans immediately following the imposed abrupt increase in ice coverage to around 50 months after onset. The initial net heat flux out of the ocean coincides with the SST ‘front’ implying that its decomposition may help interpreting its cause. We examine three periods in the evolution corresponding to the time of initial SST cooling in the subtropics (1–6 months), the progression of cold anomalies towards the ITCZ latitudes (6–15 months), and after the onset of ITCZ

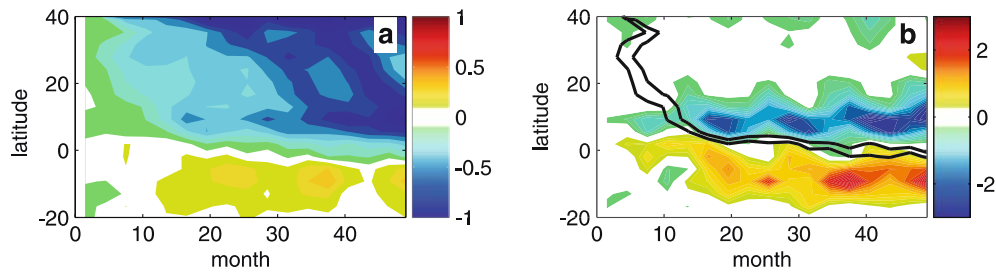


Fig. 8 Zonal mean anomalies in the transient experiment computed after sea ice onset. Anomalies are calculated from the mean of the ensemble experiments, subtracted from the mean from a control simulation. **a** SST (in K—time is in months after the onset

of the NH sea ice anomaly), **b** oceanic precipitation (in mm/day). The *dashed lines* in **(b)** are the -0.2 and -0.1 K contours of the zonal mean SST anomaly

displacement (beyond 15 months). In the initial phase (1–6 months), the rapid cooling north of 20°N (Fig. 9a) is brought about primarily by sensible heat flux north of 30°N (Fig. 9b), and latent heat flux between 20°N and 30°N (Fig. 9c). The increased sensible heat flux is caused primarily by increased air-sea temperature difference (Fig. 10a) caused by the advection of cooler air from the imposed sea ice regions to the midlatitude oceans. The latent heat flux anomaly appears to be caused by an increase in the wind speed (Fig. 10b).

Similarly, the progression of the SST front into the ITCZ region in the months 6–15 is also caused by the latent heat flux, through increased surface wind speeds (Figs. 9c, 10b respectively); note that the air-sea specific humidity difference decreases along the SST front (Fig. 10c), implying that evaporation would have been reduced if this was the sole influence. The increased wind speed originates from an anomalous north–south surface pressure gradient coupled to the SST front (Fig. 10d); the anomalous pressure gradient drives easterlies that act to increase the surface wind speeds in the northeasterly trades. The anomalous surface pressure gradient likely comes about through the reduced boundary layer air temperatures, north of the SST front, that act to hydrostatically increase the surface pressure; however, the cause is clearly more complicated as there is a distinct seasonality in the surface pressure anomalies that favor the boreal winter months. This coupling between the wind speed, evaporation, and SST, leading to an equatorward propagation of SST anomalies, is conceptually similar to the wind-evaporation-SST (WES) feedback mechanism proposed by Xie (1999), which he introduced as an explanation for the tropical Atlantic SST ‘dipole’ mode.

The ITCZ displacement occurs around month 15 when the SST front reaches the ITCZ latitudes, and the anomalous meridional pressure gradient (Fig. 10d) drives a significant southward anomalous cross-isobaric flow. The occurrence of the anomalous pressure gradient giving rise to the ITCZ displacement appears broadly consistent with the hypothesis put forward by Tomas et al. (1999) for a central role of cross-equatorial pres-

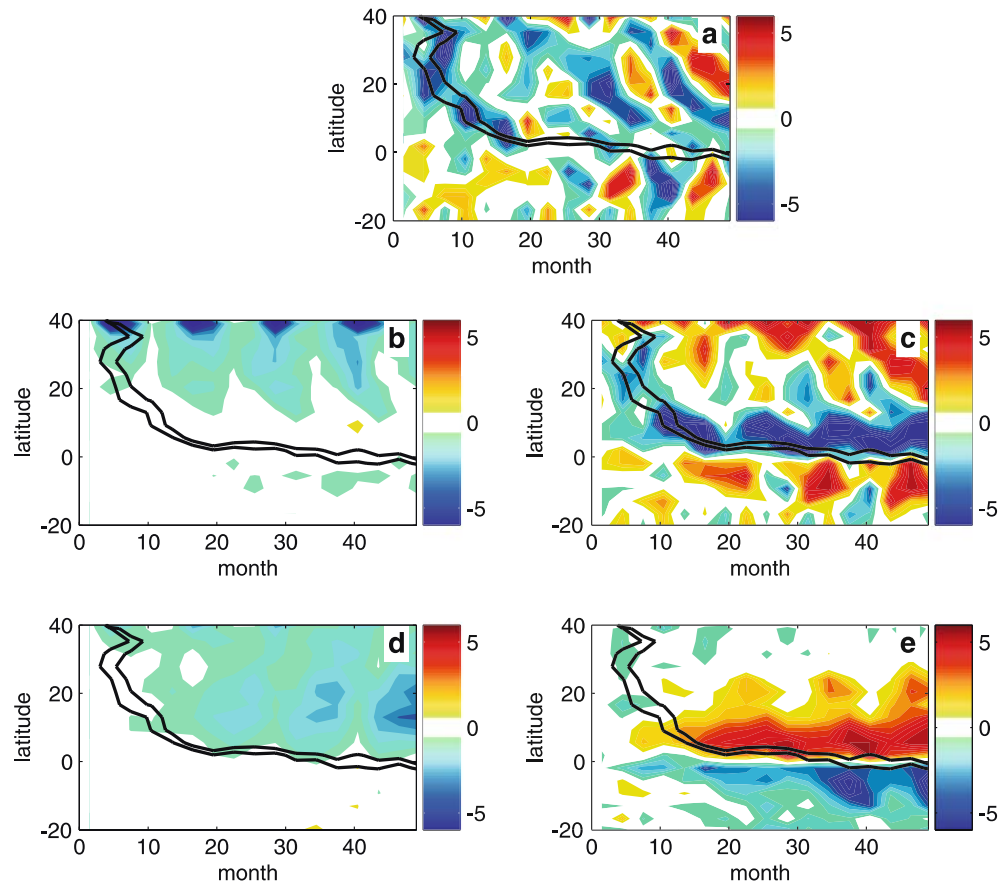
sure gradients in positioning near-equatorial convection. A significant feature of this flow is the strengthening of the tropical northeasterly trades that increase the latent heat flux to the north of the mean ITCZ position, and weakening of the tropical southeasterly trades that reduces the latent heat flux to the south of the mean ITCZ position; this is again a WES positive feedback (Xie and Philander 1994, Chang et al. 1997) that acts to maintain the meridional SST gradient and hence ITCZ displacement anomaly. A relatively weak positive feedback also comes about through the increased net clear sky radiation out of the surface (Fig. 9d) primarily through reduction of the clear sky downwelling longwave flux, a consequence of the drier tropospheric atmosphere as a result of the ITCZ displacement. These positive feedbacks on the anomalous meridional SST gradient are compensated by surface cloud radiative forcing (Fig. 9e), a consequence of the high cloud changes associated with the ITCZ displacement (Fig. 10f).

We note that unlike the permanent change to the near-equatorial wind speed after the ITCZ displacement, the WES-induced wind speed increase in the subtropics 10 – 30°N (Fig. 10b) that induced the initial SST cooling there does not appear to remain a permanent fixture. The partitioning of the fluxes over the subtropical oceans after the initial SST cooling reveals increased sensible and clear sky radiative fluxes out of the ocean balanced by a reduced cloud radiative flux (the latent heat flux contribution depends on the season). The changed partitioning of the surface flux appears consistent with that expected for a colder and drier mean climate: decreased Bowen ratio, reduced clear sky downwelling radiation due to reduced air humidity; and reduced cloudiness, primarily high cloudiness (Fig. 10e, f, respectively).

5 Proposed mechanism and interpretation

We first propose a mechanism for high latitude ice influence on the marine ITCZ based on our analysis of the simulations, after which we offer an interpretation of the model response.

Fig. 9 Surface flux analysis in the transient experiment. Anomalies are calculated as zonal averages over all ocean points. Note that the units are W/m^2 , and the color scale is the same for all panels, and positive values are into the ocean. The two black lines in each panel are the -0.2 and -0.1 K isotherms of the SST anomaly shown in Fig. 8a and indicate the leading edge of the equatorward propagating SST anomaly.



5.1 Proposed mechanism for high latitude influence on the marine ITCZ

5.1.1 STEP 1: equatorward propagation

The onset of additional northern high latitude ice reduces both latent and sensible heat fluxes to the atmosphere above, which locally cools and dries the atmosphere. This cooling and drying spreads rapidly over the entire high latitude atmosphere through transport and mixing, which in turn induces the high latitude land and ocean surfaces to cool. This cooling also similarly extends into the midlatitude oceans. Further southward communication occurs in the region of the northeasterly trades. The cooler midlatitude oceans give rise to anomalous meridional surface pressure gradients that drive anomalous easterlies in the region of the cold SST ‘front’, where the mean state winds are easterly (i.e., the northeasterly trades), the surface wind speed increases, resulting in increased evaporative cooling that pushes the cold SST front further equatorward. This is a variation of the WES feedback previously proposed by Xie (1999).

5.1.2 STEP 2: tropical marine ITCZ feedback

Once the SST front reaches the vicinity of the tropics, surface pressure anomalies associated with them intro-

duce an anomalous meridional pressure gradient across the ITCZ latitude resulting in a southward cross-equatorial flow. This displaces the ITCZ to the south, initiating positive feedback processes that keep the ITCZ southwards by maintaining the anomalous meridional SST gradient. The positive feedbacks come from the latent heat flux through altered wind speed resulting from the southward cross-equatorial flow, and reduction in the clear sky downwelling longwave flux, a consequence of the reduced atmospheric humidity. A positive surface longwave flux feedback associated with changing convection has also been noted previously by Wang and Enfield (2003). The cloud radiative fluxes (primarily due to its shortwave component) provide the negative feedback, originating from high cloud cover changes tied to the ITCZ displacement. A new equilibrium tropical SST and energy balance is reached, one that combines an anomalous southward ITCZ displacement with anomalous SST gradients (primarily cooler north—the south remains more or less unchanged) across the mean ITCZ latitude.

We note that this mechanism is consistent with the following features of the model response to an increased ice extent:

- *The relative independence of this effect on the longitude position of the imposed sea ice.* Since the entire high latitude atmosphere and surface is rapidly cooled when anomalous ice cover is imposed (because of fast

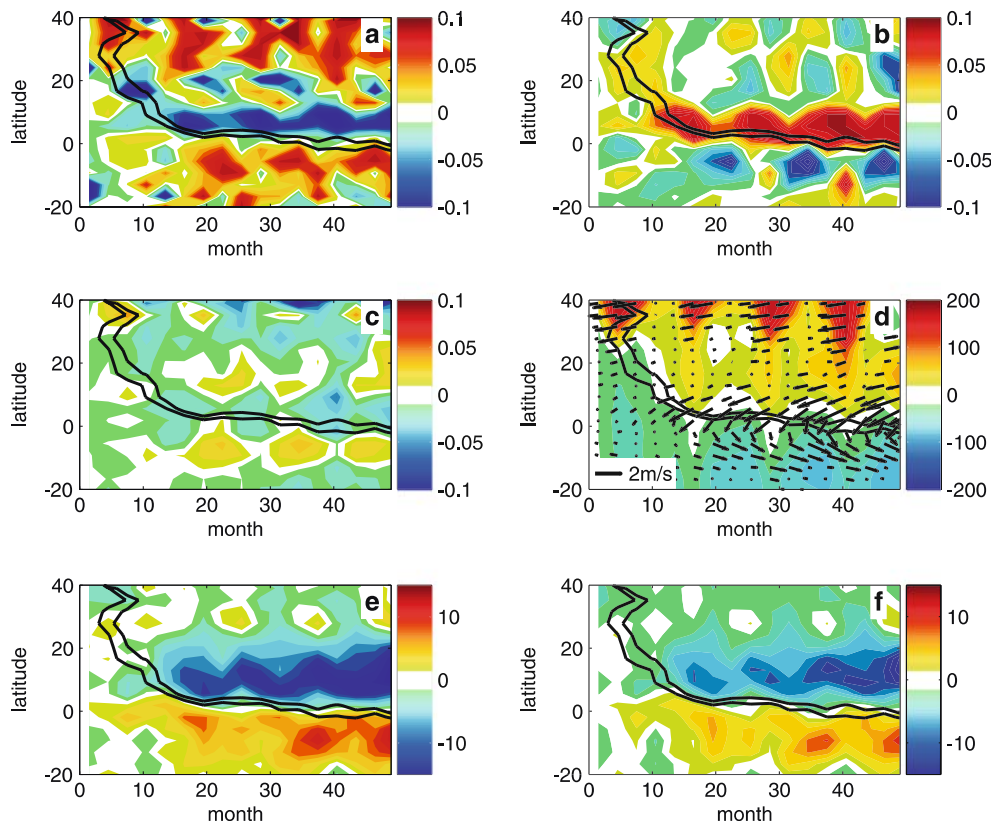


Fig. 10 Various anomalous zonally averaged fields in the transient experiment (computed over ocean points only): **a** Air-sea temperature difference expressed as a fraction of the mean air-sea temperature difference of the control simulation, **b** wind speed, expressed as a fraction of its mean, **c** Air-sea specific humidity difference, expressed as a fraction of its mean, **d** Surface pressure (Pa) and surface wind vectors, **e** total cloud cover (%), and **f** high

cloud cover (%). As with Fig. 9, the *black lines* are the -0.2 and -0.1 K isotherms of SST anomalies of Fig. 8a. Note that the air-sea temperature difference, air-sea specific humidity difference, and wind speed are expressed as fractions of their means as they give a rough indication of their relative contributions to the fractional change to the latent or sensible heat flux

atmospheric advection and mixing), the subsequent equatorward progression of the cold anomalies is independent of the longitude position of the imposed ice.

- *The coincidence of the northern subtropical SST anomalies with the northeasterly trades.* The WES feedback that is responsible for the initial equatorward progression requires a basic state surface easterly flow. Furthermore, the northeasterly trades advect cooler and drier air from the mid- and high latitudes that help maintain the cooler conditions over those regions.
- *The response to southern hemisphere sea ice anomalies.* This mechanism works equally well in the northern or southern hemisphere; we reported in Sect. 3.1 that a simulation imposing an additional SH sea ice shifted the marine ITCZ northwards in all the basins.
- *The absence of a similar ITCZ displacement over land.* The position of the ITCZ over the tropical oceans results from an interplay of meridional SST gradients, surface pressure, and the boundary layer winds (e.g., Hastenrath and Heller 1977; Xie and Philander 1994; Chiang et al. 2002) that effectively makes the ITCZ position sensitive to changes in the meridional SST

gradient. On the other hand, we conjecture that because the land is relatively dry, the latent heat flux changes that lead to anomalous meridional surface temperature gradients over the oceans do not occur over land. Also, because of the small thermal inertia over land, any land surface temperature perturbation that results from advecting drier and colder air over land is likely overwhelmed on seasonal timescales by the land response to changing seasonal insolation.

5.2 Interpretation

We argue that atmospheric humidity may be important in maintaining the hemispheric asymmetric nature of the climate response. Since water vapor is a greenhouse gas, it helps set the underlying equilibrium surface temperature so that the hemisphere with reduced water vapor content can support a lower SST than the hemisphere with higher atmospheric water vapor. We speculate that this is ultimately how the cool SST anomalies in subtropics are maintained: recall that the increased subtropical trades that initially gave rise to the cooler subtropical SST anomalies do not persist, and so wind

speed cannot be responsible for ‘pinning’ the subtropics to the cooler state. We postulate that the reduced atmospheric water vapor content acts as this ‘pin’: initially coming from passive advection of drier air from the higher latitudes into the subtropics, and later on by the change to the Hadley circulation.

If our arguments regarding the role of atmospheric humidity is correct, then a question is how the atmosphere can support a pronounced hemispheric asymmetric response in water vapor as seen in our model simulations. The answer has to do with the peculiarity in the ITCZ response—that the ITCZ displacement to the anomalously warmer hemisphere also transports moisture from the anomalously drier to the anomalously moist hemisphere (Sect. 3). So, the meridional ITCZ displacement effectively prevents dry anomalies from extending into the opposite hemisphere and allows instead the maintenance of a sharp anomalous humidity gradient at the ITCZ latitude.

From an energetics viewpoint, the ITCZ displacement can be interpreted as the required response of the model Hadley circulation in transporting atmospheric energy northwards to compensate for the loss of energy in the high latitudes as a result of the imposed ice. The increased albedo due to the imposed ice reduces the net shortwave flux at the TOA in the high northern latitudes requiring a reduction of the air temperature and humidity there to reduce OLR to compensate. However, this compensation is not sufficient and the atmosphere is required to increase poleward heat transport to those latitudes to close the energy budget. The CCM3-slab ocean model achieves this by shifting the ITCZ southwards, modifying the radiative budget to absorb more radiative flux (this comes about basically by going into a deeper convective regime). This increased energy absorption is then transported to the northern tropics by the altered Hadley circulation. Some of this energy is then lost to space in the northern tropics, but the bulk of it is transported to the northern high latitudes via increased atmospheric stationary and transient eddy transports.

6 Relevance to observed climate changes?

6.1 Present-day climate

Can we detect the influence of the high latitudes on tropics in the modern-day climate variability? We tried a straightforward data exploration, using the 1979–2002 period, where there are satellite estimates of tropical marine precipitation. To define the high latitude influence, we computed anomalous surface temperatures areally averaged from 60°N to the North Pole and subtracted them from the same but for 60°S to the South Pole. The ‘data’ we used were from the National Center for Atmospheric Research/National Centers for Environmental prediction reanalyses (Kalnay et al. 1996). To accentuate the longer-term variability, we smoothed the

resulting timeseries by applying a 13-month running mean. The timeseries (Fig. 11a), which represents variations in the interhemispheric difference in high latitude surface temperature, shows interdecadal variability with a ‘low’ (warmer SH, cooler NH) period from 1983–1992 and after 2002 (grey shaded years), and ‘high’ period before 1983 and 1993–2001. We composited the high- and low years, and subtracted the mean of the high from the mean of the low composites. The result for the precipitation field using such an analysis is shown in Fig. 11b. It shows a suggestion of ITCZ displacement in various regions—in particular, the Indian and the tropical Atlantic—and in the correct direction. The zonal mean of this response (Fig. 11c) shows this more clearly; however, the analysis remains unconvincing. An important point we emphasize is that the changes to the hemispheric difference in high-latitude temperature are quite small $\sim O(0.1 \text{ K})$ compared to the $O(1 \text{ K})$ changes seen in our model experiments—which leads us to conjecture that the influence of high latitudes on the tropics may be relatively subtle in this case, consistent with our findings.

6.2 Paleoclimate

Paleoclimate scenarios that involve significant changes to high latitude ice (more generally, hemispheric changes to temperature) are more plausible candidates for this mechanism. There is an increasing evidence to suggest that changes to the tropical climate occur associated with high latitude climate changes and in the sense demonstrated by the model. It is beyond the scope of this paper to offer a comprehensive review of paleoclimate literature in this regard (this will be the subject of a future study), but we briefly mention these paleoclimate situations where significant hemispheric asymmetries potentially came to play.

6.2.1 Unipolar glaciation during the late Tertiary

The onset of significant Antarctic glaciation occurred around 38 million years ago at the beginning of the Oligocene period, reaching its maximum volume around the late Miocene around 6 million years ago (Flohn 1981). Significant northern hemisphere glaciation and Arctic sea ice cover did not occur until around 3 million years ago. Flohn (1981) noted this highly asymmetric evolution in the earth’s climate and using the then available paleoproxy evidence, advanced the case for a hemispheric circulation asymmetry where the “meteorological equator” was displaced from its present-day position of about 6°N to about 10°N.

6.2.2 The Holocene and last glacial periods

Several high-resolution paleoclimate proxies interpreted as meridional ITCZ displacements whose behavior rel-

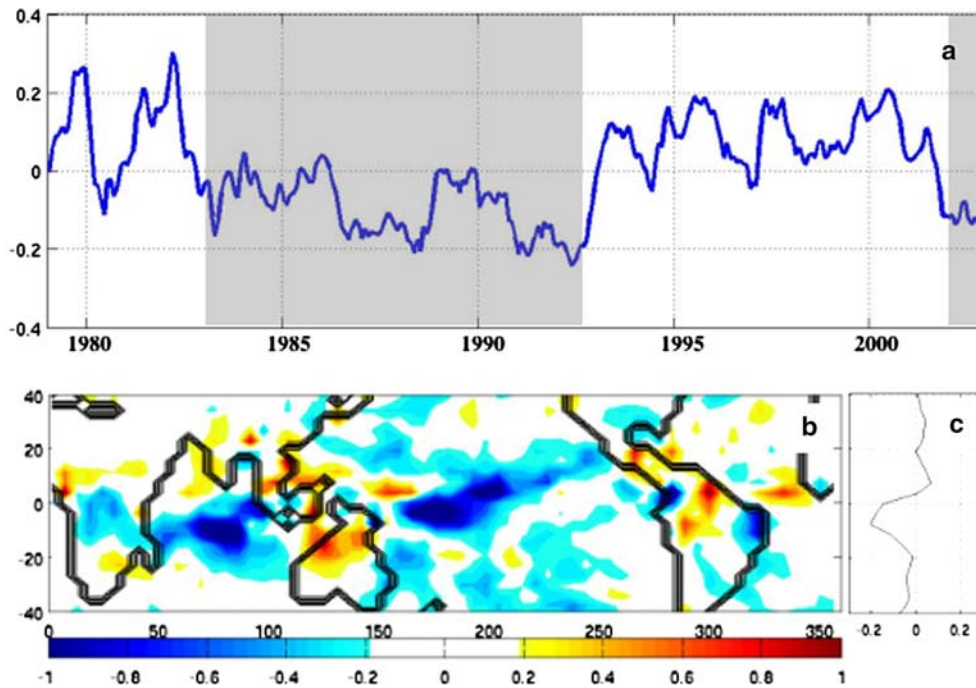


Fig. 11 Investigating high–low latitude linkages in the modern data. **a** the difference between 60°N and 90°N averaged surface temperature anomalies from the 60°S to 90°S surface temperature anomalies over 1979–2002 (see the text for details). The shaded regions define the ‘low’ index years from the ‘high’ (*non-shaded*) in

the composite analysis. **b** Annual mean composite difference of the 1979–2002 precipitation between the ‘high’ and ‘low’ years defined in (a). **c** Zonal averages of the precipitation anomalies in (b). Units of precipitation are mm/day

ative to temperature variations in the high northern latitudes (as measured by the Greenland ice cores) is broadly consistent with this mechanism. The premier example is the Cariaco basin record that shows northward (southward) shifts in the Atlantic ITCZ during warm interstadial (cold stadial) periods of the last glacial period and a pronounced shift northward during deglaciation punctuated by a return to a southward position during the Younger Dryas (Peterson et al. 2000); and also a slow drift southward from the early Holocene to the present day (Haug et al. 2001), consistent with a gradual cooling of northern hemisphere temperatures during the course of the Holocene. Koutavas and Lynch-Stieglitz (2004) offers a comprehensive review of marine ITCZ change during the last 30,000 years, and argues that north–south ITCZ variations over the Pacific, South America, and Atlantic oceans coincide with northern high latitude climate changes with warmer northern high latitude climate implying more northward ITCZ position.

We can explore the LGM situation further by examining simulations in the Paleoclimate model inter-comparison project (PMIP—Joussaume and Taylor 2000) with an interactive ocean. The question we ask is whether or not a tropical ITCZ signature of the LGM ice forcing is visible, given that the models have different parameterizations and that insolation and greenhouse gas concentrations are also changed during the LGM. The 21-Kbp insolation is generally similar to present

day, and CO₂ changes generally force a uniform cooling in the tropics (e.g., Chiang et al. 2003), so that those two effects are unlikely to directly force a significant tropical hemispheric asymmetry. The topographic and albedo effects of the northern hemisphere land ice sheets are more likely to be significant for forcing tropical asymmetry.

Figure 12 shows the LGM minus present day in annual mean precipitation in the PMIP simulations (Table 1 gives a summary of the various models and their ocean components). The tropical response varies substantially between models (note the different contour intervals for the different panels in Fig. 12), with particularly pronounced responses in the MRI2 and UGAMP model simulations. Nonetheless, the majority of the model simulations (with the exceptions being the Canadian Center and Genesis 1 models) exhibit southward ITCZ displacement during LGM. We also note that our CCM3-slab ocean model, which is updated from the CCM1 model of the PMIP simulation, shows a pronounced southward ITCZ displacement in all the three ocean basins when the full LGM boundary conditions are applied (not shown). The result suggests that, while our proposed mechanism appears to operate in a majority of the PMIP models, there is a sizable range in model sensitivity. A similar conclusion was reached by Chiang (2003) specifically comparing the tropical Atlantic ITCZ response across the PMIP model simulations of the LGM.

Table 1 The list of model data from the Paleoclimate Intercomparison Project (PMIP) and a brief description for each model. Other PMIP models were excluded either because the requisite run was not available, or because the model dynamics were not adequate to simulate ITCZ behavior

| Label | Model and resolution | Description of ocean |
|-------|--|---|
| CCC2 | Canadian Center for climate modeling and analysis model CCMA version 2 (T32 L10) | Mixed layer model |
| CCM1 | National Center for Atmospheric Research CCM1 (R15 L12) | 50 m mixed layer, fixed annual mean, zonally symmetric OHT |
| GEN1 | National Center for Atmospheric Research/Pennsylvania State University (NCAR/PSU) GENESIS 1.02A (R15 L12) | 50 m mixed layer, fixed annual mean, zonally symmetric OHT |
| GEN2 | NCAR/PSU GENESIS 2 (T31 L18) | 50 m mixed layer, diffusive OHT |
| GFDL | Geophysical Fluid Dynamics Laboratory model CDG (R30 L20) | 50 m mixed layer, prescribed seasonally and spatially varying OHT |
| MRI2 | Meteorological Research Institute model MRI GCM-IIb (4×5 L15) | 50 m mixed layer, prescribed OHT restores model SST and sea-ice amount to observations |
| UGAMP | UK Universities' Global Atmospheric Modeling programme model UGAMP UGCM version 2 (T42 L19) | Mixed layer, prescribed seasonally and spatially varying OHT restores to present-day SST |
| UKMO | United Kingdom Meteorological Office model UKMO HADAM2 (2.5×3.75 L19) | Bryan-Cox primitive equation ocean model |

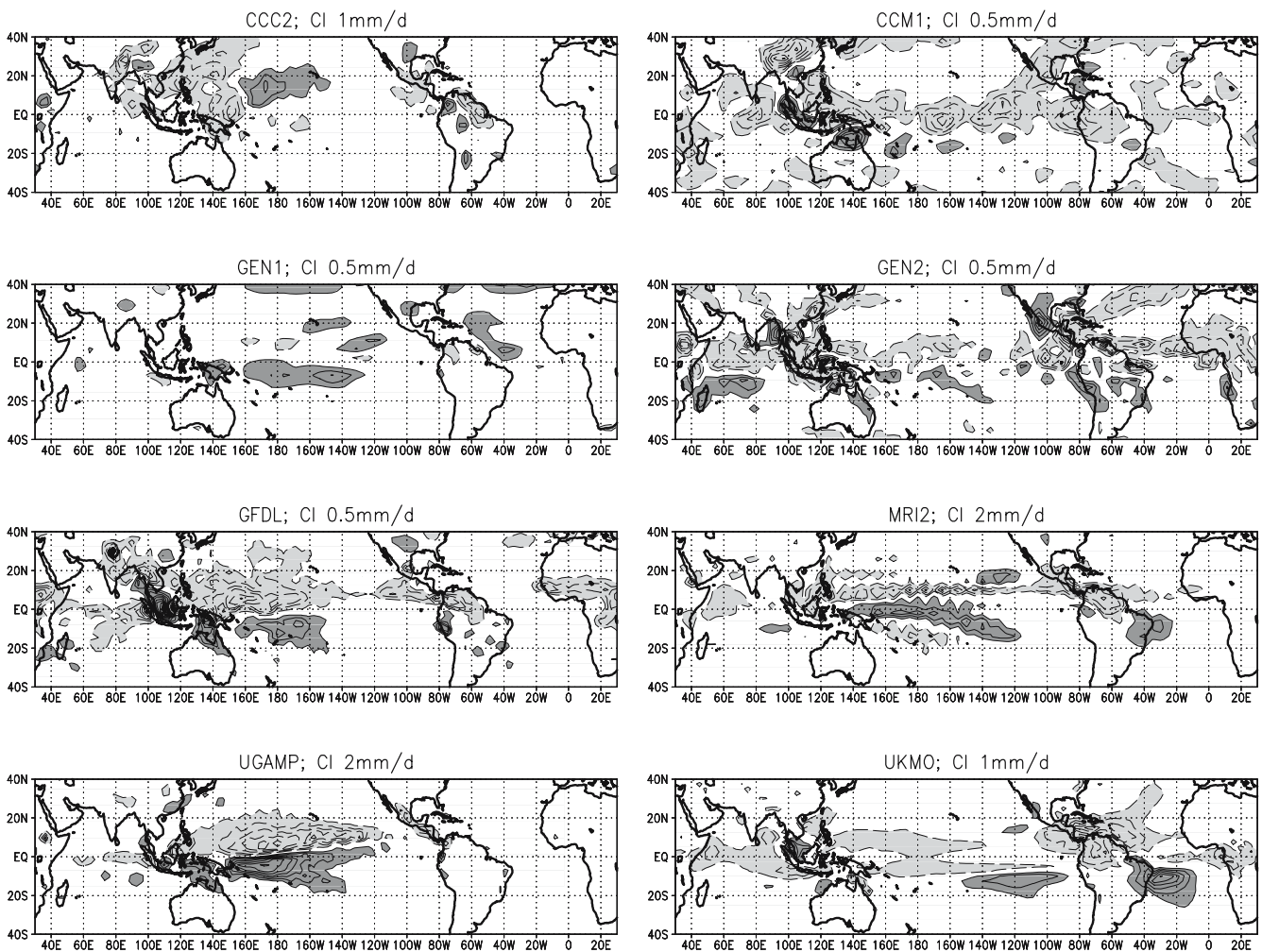


Fig. 12 Annual mean precipitation differences between the PMIP LGM and control simulations. See Table 1 for a synopsis of the various model configurations. Note that the contour intervals of the various model panels differ and are indicated on top of each panel. Positive values above the first positive contour are shaded in the

light shade, negative values below the first negative contour is in the darker shade, and the zero contour is not shown. This comparison shows that something like a southward displacement in the oceanic rainfall occurs in most model simulations, but that the magnitude of the change varies considerably across models

6.3 Discussion on applicability

The omission of interactive sea ice and ocean dynamics in our model setup may preclude a meaningful application of our mechanism to the real climate. The hypothesized influence of sea ice anomalies on the tropical climate depends on the sea ice anomalies lasting sufficiently long for the communication to reach the tropics, which according to our analysis can potentially take up to a few years (depending on the thermal inertia of the surface ocean). Also the sea ice anomalies, which we imposed in our simulations, will likely evolve given the presence of interactive sea ice physics. Simulations with interactive sea ice are a truer test for the influence of sea ice anomalies on the tropical climate, and we plan to investigate them in the future.

Ocean dynamics may change the response of the climate to high latitude ice in these ways: first, the loss of energy in the high latitudes due to the imposed ice—that we argued is ultimately compensated for by increased energy absorption by the southern tropical atmosphere through the ITCZ displacement—may alternatively be compensated for by increased ocean heat transport to the mid- or high latitudes, thus negating the need for the ITCZ to shift. Second, the ‘real’ tropical response to high latitude ice may be quite different from the simple ITCZ displacement in the CCM3-slab ocean. Tropical ocean-atmosphere feedbacks—in particular the Bjerknes feedback—may act on the forcing to bring about a very different response. Note that our model tropical SST response to LGM land ice forcing (Fig. 2b) does in fact show that the zonal equatorial SST gradient is altered—and this may act as a forcing on the Bjerknes feedback that is thought to establish the east–west zonal contrast in the equatorial Pacific. We have tentative modeling evidence to support this conjecture: when we applied the CCM3-slab ocean tropical Pacific SST anomalies in Fig. 2b to an intermediate coupled model that simulates ENSO behavior in the tropical Pacific (we used a variant of the Cane-Zebiak model as developed by Battisti (1988)) as a forcing, the intermediate coupled model responds by reducing the equatorial Pacific SST gradient even further.

7 Summary and discussion

We investigated why the CCM3-slab ocean marine ITCZ in all the three ocean basins shifts meridionally away from the hemisphere with imposed high latitude ice and altering the global Hadley circulation. We showed in particular that:

1. Land and sea ice produced similar effects on the ITCZ, suggesting that the underlying mechanism is the same for both forcings.
2. For the sea ice forcing, the impact was qualitatively similar whether the sea ice was imposed in the north Atlantic or north Pacific. Furthermore, imposed

additional sea ice in the southern hemisphere pushed the ITCZ in all three basins northwards.

3. The independence of the response to the longitude of the imposed sea ice leads us to analyze zonally symmetric responses. The anomalous zonal mean specific humidity displays pronounced interhemispheric asymmetry, with substantially reduced humidity in the hemisphere with imposed sea ice, and slightly increased humidity in the opposing tropical hemisphere. The mean meridional circulation also changes in a manner consistent with the ITCZ shift.
4. Examination of transients after the abrupt onset of northern sea ice forcing showed a southward progression of cooler SST anomalies from the imposed sea ice latitudes. Once the anomalies reached the ITCZ latitude, the resulting meridional gradient in SST thus induced shifted the ITCZ southwards.

We proposed a mechanism for the high latitude ice communication to the marine ITCZ based on our analysis. Northern high latitude ice cools and dries the atmosphere above, which in turn initiates cooling of the entire northern high- and midlatitudes through advection. A WES mechanism (Xie 1999) in the region of the northeasterly trades of the North Pacific and Atlantic oceans initiates further progression of the cold SST ‘front’ to the ITCZ latitudes. Once the cold SST front reaches the ITCZ latitudes, the meridional SST gradient thus induced initiates a southward shift of the ITCZ. Positive ocean-atmosphere feedbacks—WES, and long-wave—amplify and maintain the ITCZ displacement.

We argued that the atmospheric moisture may play a prominent role in the nature of the climate response to the high latitude ice influence. The anomalous cross-equatorial moisture transport resulting from the marine ITCZ response gives rise to a pronounced hemispheric asymmetric response in the atmospheric humidity, with drier conditions in the hemisphere with the imposed ice cover, and only small changes in the other hemisphere. The greenhouse effect of water vapor implies that the anomalously drier hemisphere also has to be cooler as a result—it ‘pins’ the climate of that hemisphere to be colder. From an energy viewpoint, the increased outgoing radiative flux lost at the imposed ice latitudes is compensated for by an increased energy flux into the atmosphere in the southern tropics, which is transported to the imposed ice latitudes through increased atmospheric heat transports, in particular by the altered Hadley circulation in the tropics, and increased stationary and transient eddy transports in the northern midlatitudes. The lack of dynamical ocean feedbacks precludes a more meaningful comparison of our proposed mechanism to the observed and inferred climate variability and change, although we argued that our mechanism may indeed be applicable in paleoclimate scenarios like the LGM where substantial hemispheric asymmetric changes to high latitude ice occurred.

We end off by discussing various intriguing implications of the results. First, our interpretation of the re-

sponse of our model Hadley circulation to imposed high latitude ice cover in balancing the global energy budget resonates with a view recently advanced by Trenberth and Stepaniak (2003) that vastly different energy transport mechanisms, in particular the Hadley and eddy transports, must be working coherently to maintain a 'seamless' poleward atmospheric energy transport. A particularly interesting statement of theirs is that "cooling by transient eddies in the subtropics is a fundamental driver of the observed Hadley circulation and realizes the seamless transport from Tropics to extratropics, while tropical sea surface temperatures over the oceans determine where the upbranch is located" (Trenberth and Stepaniak 2003). A reexamination of the model response specifically in view of their interpretation and directed towards understanding the equilibrium response, rather than the focus of the adjustment in this study, may well yield interesting results.

Our results may be germane to understanding the northward bias in the position of the marine ITCZ. This bias is usually attributed to the hemispheric asymmetry in the earth's surface boundary conditions, most notably (1) a continental configuration that puts significantly more land in the north than in the south, (2) in the eastern Pacific, a southeast-to-northwest tilted coastal geometry that promotes coastal upwelling in the south but not in the north (Philander et al. 1996), and (3) in the eastern Atlantic, the bulge of West Africa that provides a monsoonal influence over the equatorial oceans favoring the establishment of a northern marine ITCZ (Xie and Saito 2001). While the role of hemispheric asymmetric land area is commonly invoked as a possible cause, the specific mechanism of how this influences the marine ITCZ position has never been articulated to our knowledge; we wonder if what we propose is in fact this mechanism. It is not yet known what the relative importance of the above influences are on the hemispheric preference in the mean ITCZ position. However, paleoclimate scenarios may offer a possible test, since the change to the land and sea ice during LGM and during abrupt change events can be viewed as changes to the direction in the influence of hemispheric asymmetric distribution of land cover (in other words, more land to the north—considered a warming influence—changes to a cooling influence when land ice sheets occur over them).

Another climate dynamics problem that our mechanism may usefully shed light on is the global impact of the Younger Dryas, and Dansgaard-Oeschger (D/O) events during the last glacial period. These events are thought to arise from variations in the strength and position of the North Atlantic deep water formation regions that determine the North Atlantic thermohaline circulation, and the impact of these events are global—they occur not only over the tropical marine regions (as discussed in the [introduction](#)), but also over disparate regions like the Indian and Southeast Asian monsoon (e.g., Schulz et al. 1998), New Zealand (e.g., Denton and Hendy 1994), and in the Andes (e.g., Baker et al. 2001). Vellinga and Wood (2002), and Dong and

Sutton (2002) show from coupled model studies the tropical and global impacts of a simulated thermohaline circulation shutdown. A common hypothesis for how D/O events are communicated globally is through invoking altered ocean heat transports associated with the changed North Atlantic thermohaline circulation—an oceanic teleconnection mechanism. Our results suggest an alternative to the oceanic teleconnection: noting that a reduction in the thermohaline circulation likely increases North Atlantic sea ice cover (Li et al., submitted), the global impacts could be communicated via the atmospheric/surface thermal ocean mechanism proposed here. In particular, if the tropical Pacific can be induced to change as a result of the sea ice influence, the tropical feedback may result in an amplification and globalization of climate changes initiated by the change to sea ice cover.

We note that the wholesale shift of the marine ITCZ appears in other slab ocean model studies with hemispheric asymmetric forcing suggesting that the ITCZ displacement is a preferred response thereof. A prominent hemispheric asymmetric forcing relevant to present-day climate is the indirect effects of anthropogenic sulphate aerosol, whose distribution is strongly weighted to the northern hemisphere. A simulation by Rotstayn and Lohmann (2002) with the CSIRO AGCM-slab ocean model forced by anthropogenic sulphate aerosol produces a southward-shifted ITCZ. A similar result was found by Williams et al. (2001) using the Hadley center atmospheric model also coupled to a mixed layer ocean; they found in particular that feedback by the SST and sea ice was important in cooling the high latitudes and meridional SST gradient that pushes the ITCZ southwards.

The greenhouse gas forcing of earth's climate also has a prominent hemispheric asymmetric response even though the forcing itself is symmetric, with more substantial temperature increases in the high northern latitudes (Stouffer et al. 1989). Observations of sea ice extent show dramatic decreases over the last 20 years in the northern hemisphere, but insignificant changes to the southern hemisphere (Intergovernmental Panel on Climate Change Third Assessment Report, 2001: <http://www.ipcc.ch>), and projections of the sea ice response shows this asymmetry to persist. The hemispheric differential response to sea ice can potentially induce change to the tropics and in particular to the ITCZ through mechanisms proposed here. Indeed, global warming simulations by the second author (which will be reported in another study) using the Community Atmosphere Model coupled to a slab ocean and interactive sea ice model shows these effects quite prominently—a hemispheric asymmetric change to sea ice cover and tropical marine ITCZ behavior consistent with the sea ice changes.

Acknowledgements The idea to examine global climatic impacts of sea ice anomalies was first suggested to us by David Battisti, and we thank Camille Li and Andrew Friedman for their useful discussions. The model integrations were done on the IBM-SP main-

tained by the scientific computing division at National Center for Atmospheric Research (NCAR), and some of the analysis of the model output was done using the AMWG diagnostics package developed at NCAR. CMB gratefully acknowledges the support of the National Science Foundation (NSF) through grant AM0304662, and JCHC through NSF grant ATM-0438201.

References

- Baker PA, Rigsby CA, Seltzer GO, Fritz SC, Lowenstein TK, Bacher NP, Veliz C (2001) Tropical climate changes at millennial and orbital timescales on the Bolivian Altiplano. *Nature* 409:698–701
- Battisti DS (1988) Dynamics and thermodynamics of a warming event in a coupled tropical atmosphere ocean model. *J Atmos Sci* 45:2889–2919
- Broccoli AJ (2000) Tropical cooling at the last glacial maximum: An atmosphere-mixed layer ocean model simulation. *J Climate* 13:951–976
- Chang P, Ji L, Li H (1997) A decadal climate variation in the tropical Atlantic Ocean from thermodynamic air-sea interactions. *Nature* 385:516–518
- Chiang JCH, Kushnir Y, Giannini A (2002) Deconstructing Atlantic ITCZ variability: Influence of the local cross-equatorial SST gradient, and remote forcing from the eastern equatorial Pacific. *J Geophys Res* 107. 10.1029/2000JD000307
- Chiang JCH, Biasutti M, Battisti DS (2003) Sensitivity of the Atlantic ITCZ to conditions during Last Glacial Maximum. *Paleoceanography* (in press)
- Denton GH, Hendy CH (1994) Younger Dryas Age Advance of Franz-Josef Glacier in the Southern Alps of New-Zealand. *Science* 264:1434–1437
- Deser C, Magnúsdóttir G, Saravanan R, Phillips A (2004) The effects of North Atlantic SST and sea ice anomalies on the winter circulation in CCM3. Part II: direct and indirect components of the response. *J Climate* 17:877–889
- Dong BW, Sutton RT (2002) Adjustment of the coupled ocean-atmosphere system to a sudden change in the Thermohaline circulation. *Geophys Res Lett* 29:art. no.-1728
- Flohn H (1981) A hemispheric circulation asymmetry during late tertiary. *Geologische Rundschau* 70:725–736
- Hastenrath S, Heller L (1977) Dynamics of climatic hazards in Northeast Brazil. *Q J R Meteor Soc* 103:77–92
- Haug GH, Hughen KA, Sigman DM, Peterson LC and Rohl U (2001) Southward migration of the intertropical convergence zone through the Holocene. *Science* 293:1304–1308
- Hughen KA, Overpeck JT, Peterson LC, Trumbore S (1996) Rapid climate changes in the tropical Atlantic region during the last deglaciation. *Nature* 380:51–54
- Hughen KA, Southon JR, Lehman SJ, Overpeck JT (2000) Synchronous radiocarbon and climate shifts during the last deglaciation. *Science* 290:1951–1954
- Joussaume S, Taylor KE (2000) The Paleoclimate Modeling Intercomparison Project. In: Proceedings of the third PMIP workshop, WCRP report 111:271
- Kalnay E, Kanamitsu M, Kistler R, Collins W, Deaven D, Gandin L, Iredell M, Saha S, White G, Woollen J, Zhu Y, Chelliah M, Ebisuzaki W, Higgins W, Janowiak J, Mo KC, Ropelewski C, Wang J, Leetmaa A, Reynolds R, Jenne R, Joseph D (1996) The NCEP/NCAR 40-year reanalysis project. *Bull Am Meteorol Soc* 77:437–471
- Kennett JP, Ingram BL (1995) A 20,000 year record of ocean circulation and climate-change from the Santa-Barbara Basin. *Nature* 377:510–514
- Kiehl JT, Hack JJ, Bonan GB, Boville BA, Briegleb BP, Williamson DL, Rasch PJ (1996) Description of the NCAR community climate model. NCAR Technical Note TN-420+SR, pp 119–121
- Kiehl JT, Hack JJ, Bonan GB, Boville BA, Williamson DL, Rasch PJ (1998) The National Center for Atmospheric Research Community Climate Model: CCM3. *J Climate* 11:1131–1149
- Lea DW, Pak DK, Peterson LC, Hughen KA (2003) Synchronicity of tropical and high-latitude Atlantic temperatures over the last glacial termination. *Science* 301:1361–1364
- Lynch-Stieglitz J (2004) Hemispheric asynchrony of abrupt climate change. *Science* 304:1919–1920
- Manabe S, Broccoli AJ (1985) The influence of continental ice sheets on the climate of an ice-age. *J Geophys Res Atmos* 90:2167–2190
- Nobre P, Shukla J (1996) Variations of sea surface temperature, wind stress, and rainfall over the tropical Atlantic and South America. *J Clim* 9:2464–2479
- Peltier WR (1994) Ice-age paleotopography. *Science* 265:195–201
- Peterson LC, Haug GH, Hughen KA, Rohl U (2000) Rapid changes in the hydrologic cycle of the tropical Atlantic during the last glacial. *Science* 290:1947–1951
- Philander SGH, Gu D, Halpern D, Lambert G, Lau NC, Li T, Pacanowski RC (1996) Why the ITCZ is mostly north of the equator. *J Climate* 9:2958–2972
- Rotstajn LD, Lohmann U (2002) Tropical rainfall trends and the indirect aerosol effect. *J Climate* 15:2103–2116
- Schneider EK (1977) Axially-symmetric steady-state models of basic state for instability and climate studies. 2. Nonlinear calculations. *J Atmos Sci* 34:280–296
- Schneider EK, Lindzen RS, Kirtman BP (1997) A tropical influence on global climate. *J Atmos Sci* 54:1349–1358
- Schulz H, von Rad U, Erlenkeuser H (1998) Correlation between Arabian Sea and Greenland climate oscillations of the past 110,000 years. *Nature* 393:54–57
- Stouffer RJ, Manabe S, Bryan K (1989) Interhemispheric asymmetry in climate response to a gradual increase of atmospheric CO₂. *Nature* 342: 660–662
- Stuiver M, Grootes PM (2000) GISP2 oxygen isotope ratios. *Q Res* 53: 277–283
- Tomas RA, Holton JR, Webster PJ (1999) The influence of cross-equatorial pressure gradients on the location of near-equatorial convection. *Q J Roy Meteor Soc* 125:1107–1127
- Trenberth KE, Stepaniak DP (2003) Seamless poleward atmospheric energy transports and implications for the Hadley circulation. *J Clim* 16: 3706–3722
- Vellinga M, Wood RA (2002) Global climatic impacts of a collapse of the Atlantic thermohaline circulation. *Clim Change* 54:251–267
- Wang CZ, Enfield DB (2003) A further study of the tropical Western Hemisphere warm pool. *J Clim* 16:1476–1493
- Williams KD, Jones A, Roberts DL, Senior CA, Woodage MJ (2001) The response of the climate system to the indirect effects of anthropogenic sulfate aerosol. *Clim Dynam* 17:845–856
- Xie S-P (1999) A dynamic ocean-atmosphere model of the tropical Atlantic decadal variability. *J Clim* 12:64–70
- Xie SP, Philander SGH (1994) A Coupled Ocean-Atmosphere Model of Relevance to the Itcz in the Eastern Pacific. *Tellus Ser A Dyn Meteorol Oceanol* 46:340–350
- Xie SP, Saito K (2001) Formation and variability of a northerly ITCZ in a hybrid coupled AGCM: Continental forcing and oceanic-atmospheric feedback. *J Clim* 14:1262–1276
- Yang JY (1999) A linkage between decadal climate variations in the Labrador Sea and the tropical Atlantic Ocean. *Geophys Res Lett* 26: 1023–1026
- Yin JH, Battisti DS (2001) The importance of tropical sea surface temperature patterns in simulations of last glacial maximum climate. *J Clim* 14:565–581
- Yuan XJ, Martinson DG (2000) Antarctic sea ice extent variability and its global connectivity. *J Clim* 13:1697–1717